frontiers | Frontiers in Marine Science

TYPE Original Research
PUBLISHED 07 March 2023
DOI 10.3389/fmars.2023.1131543

OPEN ACCESS

EDITED BY
Dehai Song,
Ocean University of China, China

REVIEWED BY
Zi Wu,
Tsinghua University, China
Fan Xu,
East China Normal University, China
William Ross Hunter,
Queen's University Belfast, United Kingdom

*CORRESPONDENCE
Xindi Chen
chenxindi1991@hhu.edu.cn

SPECIALTY SECTION
This article was submitted to Coastal Ocean Processes, a section of the journal Frontiers in Marine Science

RECEIVED 25 December 2022
ACCEPTED 01 February 2023
PUBLISHED 07 March 2023

CITATION
Chen X, Kang Y, Zhang Q, Jin C and Zhao K (2023) Biophysical contexture of coastal biofilm-sediments varies heterogeneously and seasonally at the centimeter scale across the bed-water interface. *Front. Mar. Sci.* 10:1131543. doi: 10.3389/fmars.2023.1131543

Biophysical contexture of coastal biofilm-sediments varies heterogeneously and seasonally at the centimeter scale across the bed-water interface

Xindi Chen[1]*, Yanyan Kang[2], Qian Zhang[1], Chuang Jin[1] and Kun Zhao[1]

[1]State Key Laboratory of Hydrology-Water Resources and Hydraulic Engineering, Hohai University, Nanjing, China, [2]College of Oceanography, Hohai University, Nanjing, China

Coastal sediments filter and accumulate organic and inorganic materials from the terrestrial and marine environment, and thus provide a high diversity of microbial niches. However, sediment-based analyses typically examine bulk samples and seldom consider variation at a scale relevant to changes in environmental conditions, due to the lack of mid-long term field data which can cover both the seasonal and sediment depth variations. In this study, microbial production and bacterial community structure were determined together with grain parameters over 10 months of intertidal silty sands on Jiangsu Coast, China. We demonstrated that the microbiological effects did not merely present on the surface, but greatly varied and stratified in both physical and biological contexture within the top 4 cm layer. Bacterial community structure showed a clear vertical variation with higher operational taxonomic unit (OTU) numbers at 1~2 cm depth than in the top 2 mm, probably because of the decreasing disturbance by hydrodynamic forces. However, the microbial production rates and metabolic activities, represented by the production of extracellular polymeric substances (EPS), were always higher in the top. Seasonal changes were strongly reflected in the vertical patterns of EPS but could not explain the variation across sites. The overall EPS secretion in spring and summer was generally at high level than that in autumn and winter, with the maximum value of 5~6 times higher. Interestingly, the stratification of biological and physical properties followed a fixed relationship, where with the decrease of the grain size D_{50}, the EPS content increased exponentially, and this relationship was independent of temporal or spatial variation. Despite the significant seasonal variation of microbial activity and sedimentary grain size individually, the basic function between EPS content and D_{50} however did not alter. Filling these knowledge gaps will not only help to decipher the fate of grain-biofilm aggregates and organic matter burial under global changes, but also provide field evidence for the development of sediment transport models as well as blue carbon models incorporating microbial processes.

KEYWORDS

biofilm, intertidal sediments, extracellular polymeric substances (EPS), grain size, seasonal effects, depth profile

1 Introduction

Tidal flat ecosystems provide important services in coastal zones, such as storm protection, shoreline stabilization and food production, that support the livelihoods of millions of people worldwide (Murray et al., 2019). Various types of materials transported by tidal currents and waves, including dissolved and particulate organic matter originate from both land source and marine source (Gobet et al., 2012). Permeable bottom sediments therefore act as filters, allowing the penetration and burial of materials, and playing a central role for global carbon and nutrient cycles (Battin et al., 2003; Hunter et al., 2006; Battin et al., 2008; Zhu et al., 2022). The intertidal sediments are also constantly subjected to abiotic disturbances (*e.g.*, mixing by currents, waves, seasonal and temperature fluctuation) (Orvain et al., 2014; Passarelli et al., 2015; Hope et al., 2020; Waqas et al., 2020; Chen et al., 2021). Therefore, intertidal sediment properties and their variation in coastal area has been a great concern for many coastal engineering projects for decades, which has long been attracting the collaborative work among hydraulic and sedimentation engineers as well as ecologists.

The ecological functions of intertidal sediments are partly due to the rich microbial communities (*i.e*, microphytobenthos (MPB) mainly comprising epipelic diatoms, and prokaryotes mainly composed of bacteria) that inhabit in the permeable bottom sediments (Underwood and Paterson, 1993; Orvain et al., 2014; Paterson and Hope, 2021). The pore volume in the sedimentary bed provides high diversity of niches and supports a rich community of benthic microbial communities (Hunter et al., 2006). Some of these produce extracellular polymeric substances (EPS) to attach to sand grain surfaces (Gobet et al., 2012; Chen et al., 2017b). The natural rhythmicity of EPS production by diatom has been extensively investigated, which were reported to be well associated with its migration across the sediment-water interface in response to both internal (*i.e.*, the endogenous rhythms) and external factors (*i.e*, environmental stresses such as hydrodynamic forces and radiation) (de Brouwer and Stal, 2001; Orvain et al., 2003; Perkins et al., 2004; Chen et al., 2022). Direct microscopic observations and technologies have revealed that more than 99.9% of the bacteria live in the form of biofilms on a variety of interfaces (Donlan and Costerton, 2002).

Biofilms are defined as aggregates of microorganisms in which cells are frequently embedded in a self-produced matrix of EPS that are adherent to each other and/or an interface (Vert et al., 2012). The EPS were featured with a double-stratified structure, *i.e.*, colloidal EPS and bound EPS (Wingender et al., 1999). Colloidal EPS refer to the outer layer that are soluble in water, while bound EPS are tightly attached to the cell wall (bound EPS can be further classified into loosely-bound EPS and tightly-bound EPS, using different extraction methods). Different EPS fractions may pose distinct impact on the sediment properties. Colloidal EPS have been reported in previous study showing the potential of inhibiting desiccation by maintaining high pore water content (Orvain et al., 2003; Chen et al., 2017a). Bound EPS on the other hand are commonly related to biological cohesion, which contributes to the function of stabilizing sediment grains. In this respect, a phenomenon called "biostabilization" was defined in pioneering research as a hindered sediment erosion caused by biological action (Paterson and Daborn, 1991), which has been widely investigated in the last decades (de Brouwer et al., 2005; Lubarsky et al., 2010; Gerbersdorf and Wieprecht, 2015; Chen et al., 2019; Gerbersdorf et al., 2020; Chen et al., 2021).

The EPS bound on sediments have recently been recognized as a potential contribution to the "blue carbon" pool, which may exist for thousands of years or longer (Douvere, 2021; Valentine et al., 2021). While benthic microbes convert available carbon into microbial processed compounds along with their own biomass, microorganisms tend to attach to surfaces, therefore the microbial residues usually accumulate on mineral-associated bottom sediments (Ma et al., 2018). Once carbon is in the sediments, some of it is respired by microbes and returns to the atmosphere as carbon dioxide. However, some of the carbon stays stored, often for hundreds or even thousands of years, buried deep underground (Jiao et al., 2010; Oakes et al., 2010). The cutting-edge findings, termed as "microbial carbon pump", have illustrated the role of microbial processes in the production of recalcitrant DOM (RDOM), and RDOM, which potentially to persist for millennia, is therefore an important reservoir for carbon storage (Jiao et al., 2010). Among the three major pathways that have been identified in the microbial carbon pump, direct exudation of microbial cells during production and proliferation (*e.g.*, EPS), presents as an important contribution. For instance, among the various composition of EPS polysaccharide, the refractory components such as deoxy sugars like fucose or rhamnose are more likely to be stored (Oakes et al., 2010).

Therefore, in this study, microbial production and bacterial community structure were determined together with grain parameters over 10 months on the intertidal silty sands in Jiangsu Coast, China, to identify the main factors shaping the bio-physical contexture. We attempted to flesh out the following details that have been overlooked in previous studies, a) Does the bacterial community in coastal sediments vary stronger in centimeter-scale across bed depth than that across sites?; b) As a biofilm community, is their temporal fluctuation high/low so as to present various/similar vertical profiles?; c) Do the physical and biological properties of the bottom sediments vary correlatively or independently?. Filling these knowledge gaps will not only help to decipher the fate of grain-biofilm aggregates and organic matter burial under global changes, but also provide field evidence for the development of sediment transport models as well as blue carbon models incorporating microbial processes.

2 Material and methods

2.1 The study site

2.1.1 The location

Located between 119°30′E~122°20′E, 31°30′N~35°15′N, Jiangsu coast starts from the Xiujian River Estuary and reaches

the northern branch of the Yangtze River Estuary. Over a long stretch of the coast (approximately 1, 000 km), the accumulation of sediment from the ancient deltas of Yangtze River and Yellow River together contribute to the formation of tidal flats in this regime, forming a total land area of 32, 500 km^2 and marine area of more than 70, 000 km^2 (Zhang et al., 1999; Xu et al., 2016; Li et al., 2021). The well-known radial sand ridge system is located at the central zone of Jiangsu Coast, which supplies sediment in the coastal zone (Figure S1, also see Text S1.1 for the general hydrodynamic condition). The sediments and nutrients deposited here have not only provided extensive land resources, but also created a variety of environments which lead to different niches and ecosystems within the submerged habitats.

2.1.2 The observation site

The observation in this study was based on the previously established field station located on the tidal flat, the south of Chuandong Port, Yancheng City, central Jiangsu Coast (Figure 1A). The average tidal range measured here was about 3.68 m, and the average ratio for the flood to ebb duration (current velocity) was 0.73 (1.4) (Jin et al., 2022). The feature of the tidal flat changed seawards from vegetated flat (with salt marshes of *Spartina*) to bare flat (without vegetation). Nine observation sites were set on a profile, numbered as S1-S9 from land to sea, with S1~ S4 located on the vegetated flat, S5 on the transition, and S6-S9 on the bare flat (Figure 1A).

In this study, data collected at S6-S9 (located on the bare flat) among the nine sites were extracted for physical and biological analyses and for further comparison across sites (marked with red dots as shown in Figure 1A). The average distance between two adjacent sites was 600 m, except for S8 and S9 (about 250 m). The sediment samples collected at S6~S9 in the middle to lower intertidal zone were predominantly non-cohesive fine-grained (<200 μm in diameter) and often reworked. S6 and S7 were set in the middle of the intertidal zone, where tidal creeks were well-developed. The maximum width of the tidal creek reached 5~8 m, and the migration was significant, which greatly influenced the morphology in this area. Located in the lower intertidal zone area, the hydrodynamic forces at S8 and S9 were stronger, where ripples were formed under wave action (Jin et al., 2022). An observation datum pile was established at each site, which was used to mark the site position and to support the selection of the three points for measurement and sampling (Figure 1B).

2.1.3 The biofilms

During field observation, it was found that the biofilm covered on the surface of the intertidal tidal flat exhibited distinguished apparent characteristics in different seasons, including color, patchiness, smoothness, *etc.* (Figures 1C–E). In summer, the surficial biofilm was easy to be identified by the color of dark-brown (Figure 1E, diatom and other microalgae or phototrophic bacteria as the dominant, which reflected high chlorophyll concentration), where separate "clusters" or "patches" were connected to form a covered area with a clear boundary (Figure 1C). A close examination showed that the glue-like biofilm layer smoothed the bed surface. After removal of the film, the muddy layer underlain was exposed, in the color of light brown (Figure 1E). In contrast, the biofilm in winter was different (detected by naked eyes), presenting in small fractions of mushroom-like structures, and in the color of gray and white (Figure 1D). The feature of the diatom biofilm observed in summer faded, mainly due to the low temperature, which was replaced by the bacterial-dominated biofilm. Only local colonization was observed in

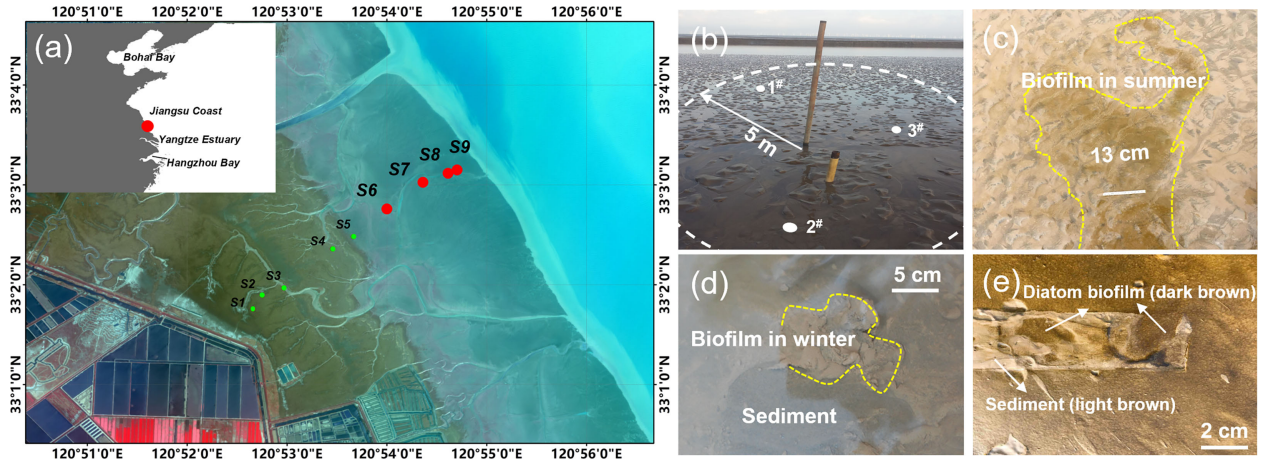

FIGURE 1
The sampling sites. **(A)** The location of the four sampling sites, among the nine long-term observation sites previously established, numbered of S6 to S9 from land to sea, on the intertidal flats in Jiangsu Coast. Inset - position of the Jiangsu Coast. **(B)** A site marker set at S9, in a radius (*R*=5 m) around which three points were randomly selected for sampling. **(C)** Biofilm formed a patch on the surface of the bottom bed (photos taken at S6 in summer). A paper ruler was place on the bed (13 cm in length) as a scale marker. The biofilm in winter was featured by small fractions of mushroom-like architecture, and in the color of gray and white **(D)**, while a smooth and glue-like thick layer in dark brown was observed in summer, with diatom as the dominant **(E)**. Removal of the ruler uncovered the underlain sediment layer which showed in light brown **(E)**.

winter (Figure 1D), compared to a globally distributed pattern in summer (Figure 1C). This indicated that seasonal change caused a transition from confluent and compact biofilms to sparsely colonized surfaces with heterogeneous biofilms.

2.2 Sample collection and analytical method

2.2.1 Sediment sampling

Field observation and sample collection were conducted at S6-S9 mentioned in Section 2.2, every 1-2 months from November 2015 to August 2016 (Table 1). Samples were all taken during spring tide when the flat was exposed. Three sampling points were randomly selected for each site in a R=5 m circular experimental area, delimited by the datum pipe set at the center. Depth sediments (including the very surficial "fluffy" layer) were extracted undisturbed from the bottom bed using sediment cores. A sediment core with a depth of 4 cm and diameter of 5 cm was taken at each sampling point. Depth profile was obtained by scaling the core into 6 layers, instead of achieving depth-averaged properties, for both the physical and biological parameters (freezing-cut method was applied for the stratification, see Table 1 for the detailed information). The sampling depth was 4 cm, which was referred to the change of tidal flat surface elevation without considering the extreme weather and the large-scale erosion and sedimentation caused by creek migration. In addition, since the depth profile of EPS naturally presented a distributive property with a high concentration in the top 1 cm layer and a rapid decay within a few centimeters of depth, this study did not involve EPS data at deeper layers. Besides, the scaling was not uniform, but dense-to-sparse from top to down. In rippled area, the cores were taken at the crest, leaving the trough which was filled with water even during exposure. After stratification, the samples collected from three randomly selected sampling points at each site were placed in the same container (50 mL plastic centrifuge tube), defrosted, and stirred to obtain a uniform mixture for further analysis.

2.2.2 Grain size measurement

The grain size distribution of the sample was measured by Malven-Mastersizer3000, a particle size analyzer based on the laser diffraction principle. The measurement range was 0.01~3500 μm. The data acquisition speed was 10 kHz, and the repeatability error was less than 0.5%. The particles were further dispersed in water in the main container for measurement (wet method) when the function of ultrasonic dispersion was turned on. It was employed to ensure the full dispersion of sediment particles when the sample contained fine particles (aggregated of fine mineral grains or organic matters), to improve the measurement accuracy.

TABLE 1 Sampling date and core scaling.

Date	Vertical stratification (cm)	
14/11/2015 (Autumn)	Each core was scaled into 6 layers. Taking S6 as an example (the depth from the surface):	S61: 0.0~0.2 cm
24/12/2015 (Winter)		S62: 0.2~0.5 cm
25/02/2016 (Winter)		S63: 0.5~1.0 cm
24/04/2016 (Spring)		S64: 1.0~2.0 cm
19/06/2016 (Summer)		S65: 2.0~3.0 cm
19/08/2016 (Summer)		S66: 3.0~4.0 cm

2.2.3 EPS extraction and analyses

The extraction of EPS followed the protocols proposed by (Li et al., 2008; Liang et al., 2010). The stratified EPS was extracted in the order of colloidal EPS, loosely bound EPS (LB-EPS), and tightly bound EPS (TB-EPS), respectively. Sediment sample (3 mL, defrosted) was placed in a 50 mL centrifugation tube. Sterile deionized water was added to suspend the sediment to a total volume of 30 mL. The tubes were then centrifuged (3,000 g, 15 min, 4°C). The supernatant was collected and then further centrifuged (13,200 g, 10 min, 4°C) to ensure a complete removal of the suspended solids. The supernatant contained the colloidal EPS. The bottom sediments were resuspended to 30 mL with sterile deionized water and then added with 0.18 mL formamide (37%) (Sunil and Lee, 2008). The formamide was added to protect the cells and to prevent the leak of intracellular matters. The mixture was placed in an orbital shaking incubator and run for 60 min (150 rpm), after which the suspension was centrifuged (5,000 g, 15 min, 4°C) and filtered through 0.45 μm filters to collect the LB-EPS solution. Bottom sediments were resuspended with an extraction buffer (2 mM Na_2PO_4, 4mM NaH_2PO_4, 9mM NaCl, and 1 mM KCl, pH 7) to 30 mL, and added with 70 g/g VSS of gel cation exchange resin for the extraction of TB-EPS. The tube was again oscillated (150 rpm, 60 min) in the shaking incubator. Then the supernatant was centrifuged at high speed (10,000 g) for 15 min first and filtered through 0.45 μm filters, to collect the TB-EPS solution. All the EPS solution was stored at -20°C for further analysis of different components.

As the main components of EPS, polysaccharides and proteins were examined respectively (Gao et al., 2008). Anthrone method was applied for the measurement of polysaccharide content in EPS, using glucose as the respective standards (Raunkjaer et al., 1994). EPS-protein was measured following the Lowry method, using bovine serum albumin as the standards (Lowry et al., 1951). Several sediment samples were selected for obtaining the scanning electron microscopy images (SEM, HITACHI S-3000N, 25 kV). Here, note that freeze drying method was used for sample preparation, therefore while the presence of EPS in SEM images can provide evidence of the matrix structure, such images must be viewed with caution when interpretating the biofilm-sedimentary micro-morphology because the sampling process is destructive (Perkins et al., 2006).

2.2.4 Bacterial community

The microbial community structure analysis was determined *via* 16S rRNA amplicon sequencing (Magigene, Guangzhou, China). PCR amplification, purification, pooling and

pyrosequencing of a region of the 16S rRNA gene were performed following the procedure described by (Fierer and Jackson, 2006). The community DNA of microbes was extracted using a FastDNA Spin kit (Bio 101, Carlsbad, CA, U.S.A.). Raw pyrosequencing data were processed using Mothur (Schloss et al., 2009) and QIIME (Caporaso et al., 2010) software. Operational taxonomic units (OTUs) were identified with uclust at the 97% sequence similarity level (Edgar, 2010). Beta diversity (unweighted UniFrac distances) was calculated based on a randomly selected subset sequences per community. See Text S1.2 for the statistical analyses.

3 Results and discussion

3.1 Grain size distribution

The distributive patterns of sediment grain size in winter (Figures 2A–D, left column) showed obvious peaks for all the four sites, indicating that the beds were more homogeneous in components where the grain size was mainly concentrated within the range of 50 to110 μm (classified into coarse silt or fine sands), compared to the summer patterns (Figures 2A–D, right column). Except for S73, S74 and S75, the content of fine particles (<16 μm, including fine silt, very fine silt and clay) in other sediment samples was relatively low (<20%). It is interesting to note that the content of fine particles in the very surficial ~mm layers was low (*e.g.*, S71 and S72), but increasing in the subsurface layer (0.5~3.0 cm depth from the surface, *e.g.*, S73~S75).

The summer patterns changed greatly, especially for S6 and S7 (Figures 2A, D), where cohesive particles became dominate. For instance, more than 80% of particles for S61 had the grain size less than 30 μm in summer, compared to the cumulative volume less than 10% of that in winter. The D_{50} for S61 decreased largely from 67.9 (winter) to 8.2 μm (summer). The distributive pattern became flat, indicating that the heterogeneity increased. This phenomenon was observed not only for the very surficial layer, but also for the sublayers such as S62, S63 and S64 (the top 2 cm), while the cumulative curve gradually retreated to the winter profile for S65 and S66 (2~4 cm). Similar variation occurred for S7. However, the "finer trend" became less obvious for the sites at seaside (*i.e.*, S8 and S9). This means that the bed at landside exhibited stronger potential in capturing and fixing fine particles in summer.

By comparing the seasonal effects in the grain size distributive patterns across S6~S9, S8 and S9 were less affected, indicating by the similar patterns for each layer, despite noted increase in the proportion of cohesive particles (<30 μm) in summer samples. In contrast, the distribution for S6 and S7 changed significantly. This showed that seasonal effects on the grain size distribution of the bottom bed (4 cm in depth) decreased from land to sea in the study area.

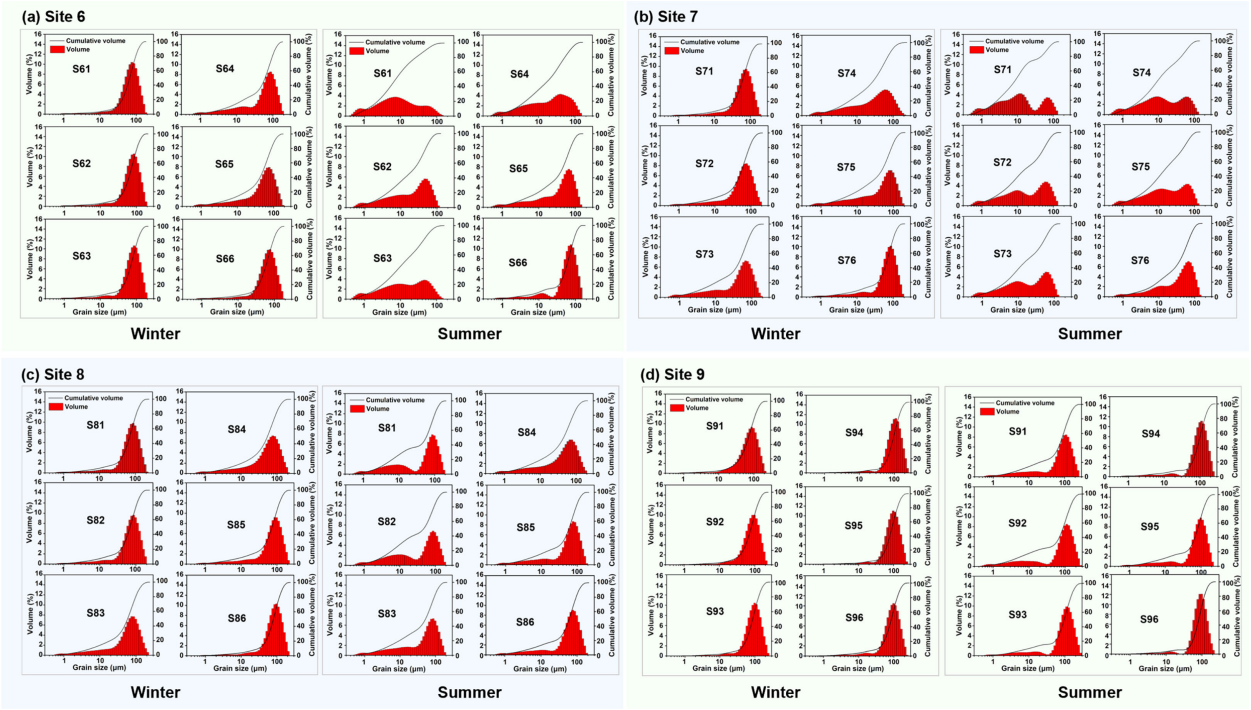

FIGURE 2
Grain size distribution of sediment examined at different layers (1~6) of the sediment cores collected at different sites (S6~S9) **(A–D)** in winter (left) and summer (right). Seasonal effect was more obvious on reshaping the distributive curve for Site 6 and Site 7 than the seaward sites (S8 and S9). The first notation represents the site number and the second for the layer, *e.g.*, S61 represents the top layer of the sediment core collected at Site 6. The winter data were collected on 24 December 2015, and the summer data on 19 June 2016.

3.2 Diversity of bacterial community

Cluster analysis of species abundance was performed for selected samples (2 samples from layer 1 and layer 4 for each site), which was used to represent the community composition and abundance of groups of samples at a certain taxonomic level. Abundance was represented by color shade and the samples were clustered by abundance and composition. In this study, species abundance was clustered at phylum level, as shown in the heatmap (Figure 3A). The value of the relative abundance of each row of species was standardized. The abundance for S6 was very low in each classification, while the abundance for S8 and S9 (S84 and S94) was relatively high. Although the abundance in the top layer of S7 (S71) was very low, the species abundance in the sublayer (S74) largely increased.

Beta diversity concerns the differences of biodiversity among samples. Based on the unweighted Unifrac distance matrix, the samples were cluster by UPGMA method, and the results were integrated with the species relative abundance of each sample at the phylum level (Figure 3B). The branch distance represented the similarity of the species composition of the compared samples. Results showed an obvious characteristic of S6 with dominant bacteria of *Proteobacteria*. The diversity increased from land to sea, showing an overall trend of S91>S81>S71>S61. The increase of hydrodynamic conditions may possibly explain this. In the sub-intertidal zone, the material exchange was frequent, where sediments from different regions attached with different dominant species were strongly mixed in the water column. During calm period, the aggregates of sediments along with their bound organic matters and microbial communities settled down, and become part of the bed, where the new sediment-water interface was formed. This can result in a recombination of microbial communities and competition due to the rapid change of the micro-environments. In addition, by comparing the depth data, it was found that the diversity increased with depth (S64>S61, S74>S71, S84>S81, S94>S91), which was consistent with all four observation sites.

Further analysis showed that S84 and S94 were similar in the community types at the phylum level (Figure 3B). Similarly, the structural composition of S81 and S91 was closed, but the distance between S94 and S91 was greater. The large component of *Firmicutes* found in other samples (except for S61) was, however, difficult to be detected in S84 and S94, while *Chloroflexi* and *Actinobacteria* obviously increased instead. This may also be ascribed to hydrodynamic effect and frequent rework of sediments occurred at the sediment-water interface (Wu et al., 2023). As a result, the sediment that originally covered the surface and had similar composition of the colonies was eroded and transported. The sediment that was brought by the tidal current from other areas and contained colonies that were different from the local community would be deposited on the tidal flat. Therefore, the community was greatly stratified within the first millimeters due to the frequent exchange of materials by stronger hydrodynamic forces in the lower zones.

The microbial community in the sediments presented great heterogeneity both vertically and horizontally, but the changes along depth were more evident. The comparison of samples across sites showed that the abundance and diversity of colonies increased significantly with the increase of offshore distance, indicating that

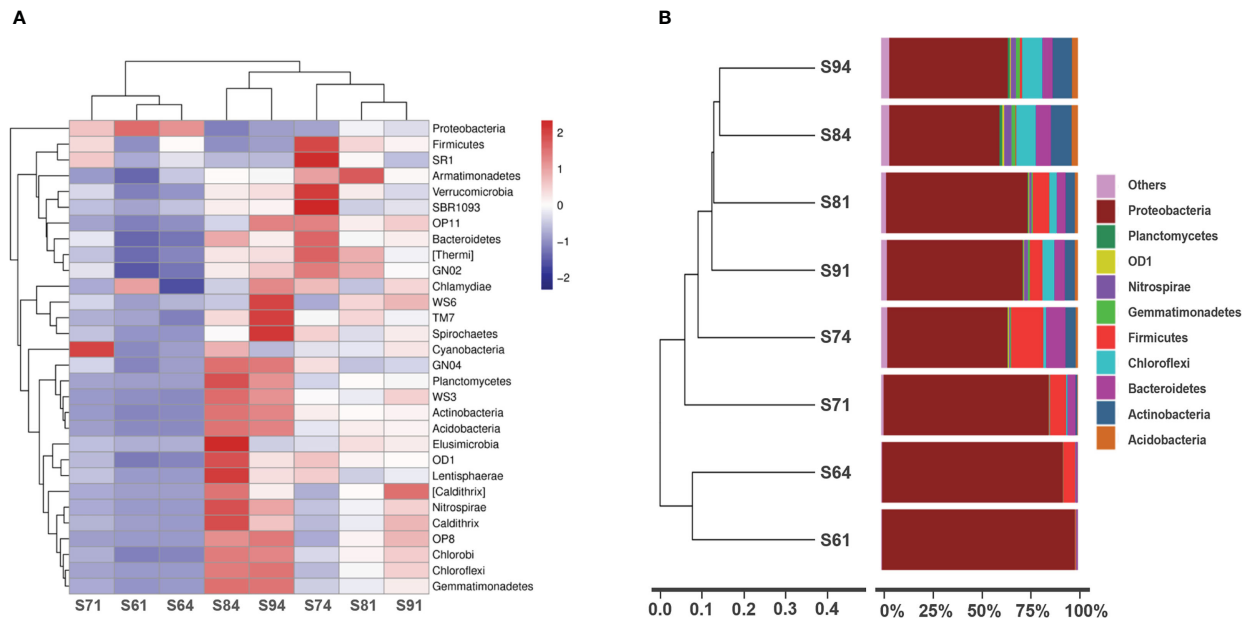

FIGURE 3
Cluster heatmap (phylum level) for community analysis **(A)** and relative abundances (percent) of dominant lineages **(B)** in sediment cores of selected layers (*i.e.*, the top and the 4th layer at each site, 8 samples in total). **(A)** Samples were represented horizontally, and species were represented vertically. The species were clustered on the left and the samples were clustered on the top, reflecting the similarity of community composition among samples. **(B)** The results were clustered on the left to obtain the UPGMA tree based on unweighted Unifrac distance (phylum level). The legend in the bottom left corner represents the distance scale.

appropriate inundation and hydrodynamic forces (which created more complex environment and material exchange) favored the increase of microbial diversity. Although the physicochemical gradients across the sediment-water-interface usually occurred at the μm or mm scale reported in previous studies (Mcclain et al., 2003; Cai et al., 2022), a stratified microbial community was observed in this study. Our results showed that the distribution of microorganisms in the intertidal bottom bed was not only concentrated within the interface scale, on the contrary, the relative abundance increased deeper into ~cm downward from the surface.

3.3 The micromorphology of sedimentary grains

The particles generally featured as separated mineral grains (Figure 4A, ×150), but biofilms (appeared as white, floc-like substances) were also observed locally adhered to the grain surface (indicated by the red circles, Figure 4A). A zoomed-in image showed the clear micro-morphology of the aggregates, where a visible diatom cell, with *Bacteroidetes* cells (of much smaller size compared to the diatom) in the surrounding, and their secreted EPS, were found tightly attached/trapped in the "gully" of the outer surface of the mineral grain (Figure 4B, ×1, 000).

This indicated that even in winter when biological effects were less significant as previously thought, SEM images of sediment samples provided robust evidence demonstrating that there was still non-neglectable microbial information ("footprints") incorporated in the sedimentary environment.

A three-dimensional network structure formed by the interweaving of biofilm-sediment particles was clearly observed in the sample collected at S8 (Figure 4C, ×800). Fine particles (d< 30 μm) were embedded in the matrix. While EPS "bridged" and connected individual fine particles, the particles themselves also performed as the skeleton of the matrix. The microbial-abiotic interactions together contributed to the final establishment of such complex network structure formed by both biotic and abiotic elements. In addition, small patches of biofilm were observed locally on grains (Figure 4C).

3.4 The vertical distribution of EPS

Seasonal effects on microbial metabolism in the sedimentary bed were investigated by comparing the depth profile (4 cm from the surface) of EPS in Autumn/Winter and Spring/Summer at S6~S9 (Figures 5, 6).

The overall EPS contents for all sites were low in Autumn/Winter, with an average total EPS content of about 100 μg/g.DW (Figure 5). Different from traditional knowledge, EPS was not only concentrated at the millimeter scale, but exhibited a certain content in all the six stratified layers, and the vertical distribution was relatively uniform (Figures 5A–C, changed from 60~150 μg/g.DW for all the 69 samples). Moreover, the maximum EPS layer content did not exist in the top layer though, but in the sub-surface layer at the depth of about 1.5~2.5 cm below the surface. This may be related to the fact that in Autumn/Winter there were mainly bacterial biofilms instead of microalgal biofilms due to the low temperature. Unlike benthic microalgae, most bacterial community do not rely on photosynthesis to sustain their growth, therefore, they successfully survive in the pores of the sediment extended deeper into the bed. As the sub-layer was protected by the overlain sediments without being directly disturbed by the flow, the EPS was accumulated and preserved.

In contrast, the vertical profiles of EPS varied greatly in Spring/Summer, but the variation was rather different across sites (Figures 6A–C). The overall EPS content at S6 and S7 were relatively high, compared to S8 and S9. Taking S7 sampling in April 2016 as an example, the EPS content in each layer reached about 200 μg/g.DW (Figure 6A), which was twice as high as that in Autumn/Winter (Figure 5A). However, the EPS for S6 and S7 showed obvious heterogeneity in vertical distribution, where highly concentrated EPS was distributed in the top 2 mm layer (Figure 6B). The surficial EPS content reached up to 650 μg/g.DW (S6) and 450 μg/g.DW (S7), 4~6 times of that in Autumn/Winter (Figure 5B). Meanwhile, the content in the sub-layer (0.2-0.5 cm from the surface) decayed rapidly to lower than 300 μg/g.DW, and to 100~150 μg/g.DW for S66 and S76 (3~4 cm from the surface), less than 1/4 of that in the top-layer (Figure 6B). In contrast, the

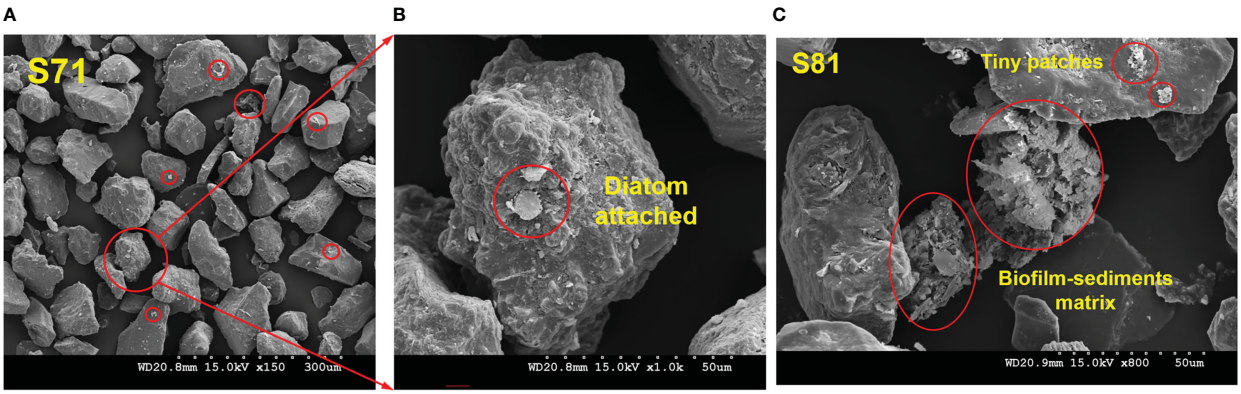

FIGURE 4
Scanning electronic images showing the micromorphology of the biofilm-sedimentary aggregates. Sediment samples were collected at S7 **(A, B)** and S8 **(C)** in winter, 2016.

average EPS levels for S8 and S9 (Figures 6A–C) did not increased significantly compared to the Autumn/Winter condition (Figures 5A–C). The contents for each layer were closed, with little change along the depth, which was quite different from the highly stratified vertical profile shown for S6 and S7.

This phenomenon may be related to the abundance of benthic microalgae changing in different seasons. In Spring/Summer, temperature, radiation, and other environmental conditions favor the colonization of microalgal biofilms. S6 and S7 were located above the average low tide line, where the exposure duration was longer compared to S8 and S9. As a result, biofilms at S6 showed explosive growth in June (see Figures 1C–E). As the growth of microalgae was also limited by the light condition, the large accumulation of EPS was not found deeper inside the bed. Consequently, the highly concentrated EPS only spread over the first ~2 cm, which was sensitive to depth, resulting in a rapidly decayed vertical profile. For S8 and S9, the exposure of benthic microalgae was inhibited due to partly inundation at high tides. Therefore, changes in the overall EPS content at S8 and S9 sites were relatively small even in Spring/Summer. The decrease of EPS level in August (Figure 6C) can be explained by the grazing pressure, when crabs and other benthic fauna (bioturbation) feeding on the bottom microalgae bloomed in these months (crab burrows can be observed in a large density).

Comparison across sites showed that seasonal effects on the vertical distribution of EPS within the depth of 4 cm of intertidal bottom sedimentary bed decreased with the increase of offshore distance, which was consistent with the seasonal variation of grain size distribution characterized in Section 3.1.

3.5 The correlation between EPS content and grain size

The grain size (represented by D_{50}) along the depth varied correspondingly with the EPS profile (Figure 7, taking the sample collected in the summer of 2016 as an example). The total EPS was represented by the sum of EPS polysaccharide and EPS protein which were two main fraction of the production. Although D_{50} and EPS profile showed obvious seasonal variations respectively, the trend between the two profiles was closely related. The vertical profile of D_{50} showed opposite trend against EPS profile across our four observation sites.

Further analysis based on 123 sampling results, the EPS content in bottom sediment exhibited tight relationship with the change of the grain size (D_{50}), presenting a negative correlation (Figure 8). With the increase of grain size, the accumulation of EPS in sediment decreased rapidly, fitting a negative power relationship (R^2 =0.74). This indicated that the appearance of high concentration of EPS on the tidal flat almost occurred synchronously with the attraction of fine sediments in field. This relationship hints that the potential of biofilm colonization on fine sediment may be much higher than that on coarse grains. Researchers have pointed out that diatoms were more observed in muddy sediments, although there was something of a chicken and the egg situation (Fagherazzi et al., 2013). It remains as open questions that do diatoms preferentially live in muddy sediments, or do they strip the fine grains from water column and enhance the retention? Or, other than that, both are true and a positive feedback triggered much matters. The accumulation of EPS in the sedimentary bed may increase the cohesion and adhesion of the interface, which helps further capture and fix fine particles in the bed. The erosional resistance for fine sediments settling on the flat increases through consolidation, which may need a long calm period to complete such process (Amos et al., 2003; Stone et al., 2008). This means that the newly deposited fine grains may be easily re-suspended under tidal currents. But with biological cohesion, surficial biofilms may increase the initial attachment and successive retention of deposited particles (especially fine particles) (Battin et al., 2003; Battin et al., 2016; Roche et al., 2017). Early research has proved that with favorable environmental conditions, diatom can secrete a large amount of EPS in a very short period (*i.e.*, a few hours), which may well explain the relatively high EPS concentration observed in the top layers in Spring/Summer in this study (Paterson, 1989). Therefore, the quick secreted EPS can further

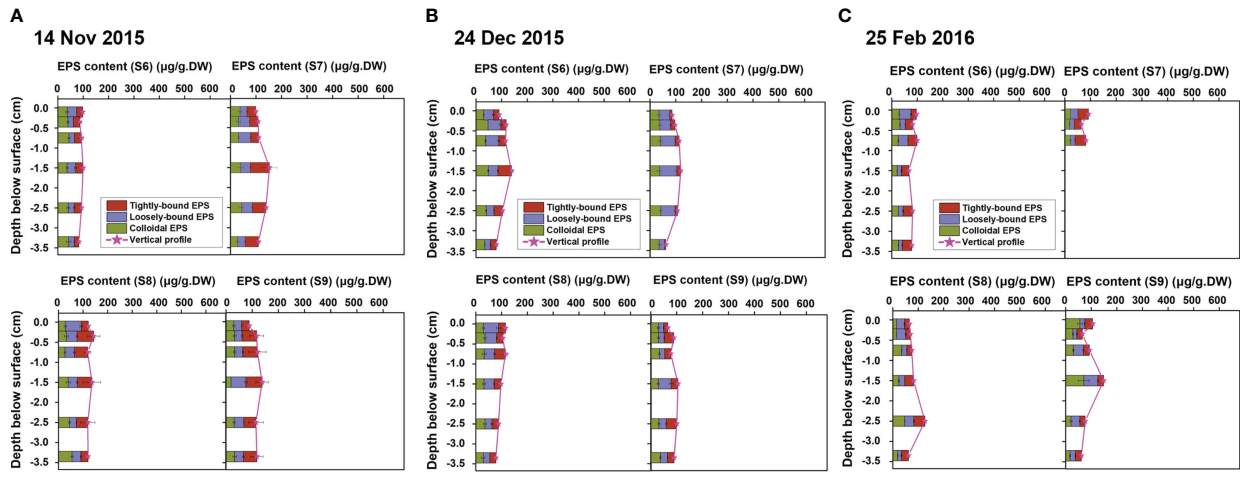

FIGURE 5
Vertical profiles of EPS (represented by stratified EPS of tightly-bound EPS, loosely-bound EPS and colloidal EPS) in the sediment samples collected at S6~S9 in Autumn and Winter, in November 2015 **(A)**, December 2015 **(B)** and February 2016 **(C)**, note that data were missing for S74~S76).

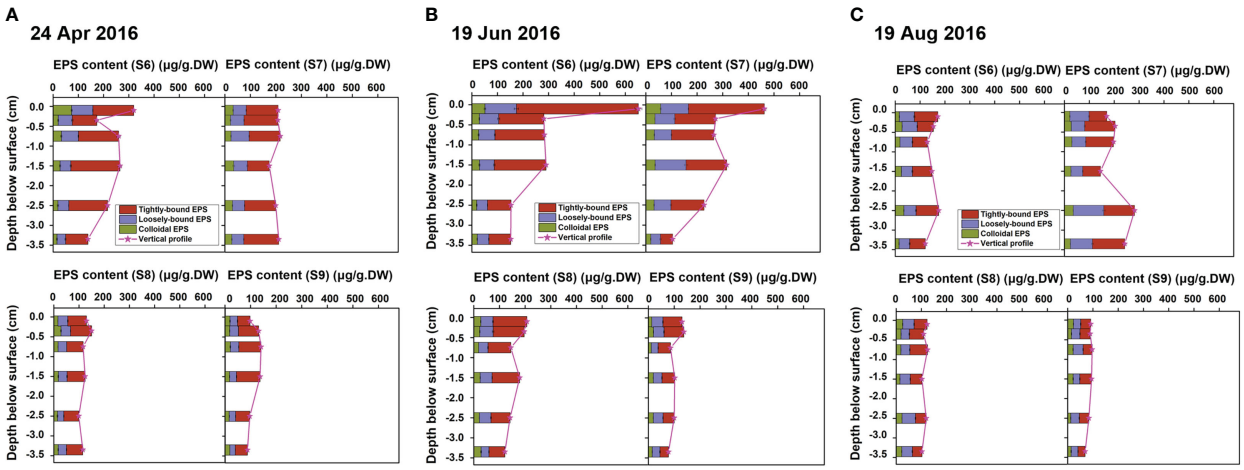

FIGURE 6
Vertical profiles of EPS (represented by stratified EPS of tightly-bound EPS, loosely-bound EPS and colloidal EPS) in the sediment samples collected at S6~S9 in Spring and Summer, in April 2016 **(A)**, June 2016 **(B)** and August 2016 **(C)**.

wrap and embed the particles and make them as parts of the EPS matrix away from being eroded individually.

This result provides evidence when biofilm factors should be carefully considered into numerical models when investigating sediment transport, morphological evolution, and ecological mechanisms. The parameterization of EPS can be expressed by the function related to the grain size which has been commonly used by sedimentologists and modelers.

However, it should be noted of the possible effects or limitations of the scale issue, regarding to the thickness of 4 cm layer compared to the natural erosion and deposition that may occur during a period of 10 months. Therefore, the possibility that the tendency showed in Figure 8 could be just that the biofilm and sediments both changed in tandem with the seasons, or should they physically be linked to show a symbiosis effect, awaits to be further investigated.

4 Implications

Biologists working on biofilms have commonly concentrated on the very surficial layer, as biofilm was only thought to form on the surface (without considering the penetration downwards inside the bed), and the thickness of biofilm within ~10^{-4} m to ~10^{-3} m was considered. In contrast, variation at a relatively larger scale over a depth of ~10^{0}m to ~10 m was concerned for most coastal engineers and sedimentologists. We demonstrated that the microbiological effects did not merely present on the surface, but greatly varied in both physical and biological contexture within the top 4 cm layer. This active layer, incorporating with photoautotrophic communities of cyanobacteria and algae that co-occur with heterotrophic bacteria, provide critical functions in many ecosystems. First, these communities play an essential role in biogeochemical cycling. As the pioneering settler on Earth, they increase biodiversity, fix atmospheric carbon (C) and nitrogen (N) (Elbert et al., 2012). And through metabolism they produce organic matter, which is subsequently partly stored in the bed in the form of EPS carbohydrate and protein, as investigated in this study. This contributes importantly to the "blue carbon" that the wetlands can hold as a main source to RDOM, which potentially to persist for millennia (Jiao et al., 2010). Fossil records also suggest that photoautotrophic surface communities like today's components formed the earliest terrestrial ecosystems over three billion years ago (Rodriguez-Caballero et al., 2018). This together indicates that the surficial biofilm-sedimentary layer has long influenced Earth's ambient conditions, affecting processes such as weathering, oxygen accumulation in the atmosphere, carbon sequestration and other major biogeochemical cycling.

In addition, this layer may also control sediment infiltration due to bio-mineral aggregates filling the pores (also known as bio-clogging) (Thullner and Baveye, 2010; Rubol et al., 2014; Volk et al., 2016). Within this matrix, water is found as the dominating component. However, despite 99.8% of the water shared the similar properties with the bulk water, only a small amount of EPS (0.2%) components can reduce permeability significantly (Vogt et al., 2000; Gerbersdorf and Wieprecht, 2015). Meanwhile, water retention can be increased on the other hand, by inhibiting evaporation in the face of high temperature and drought as the changing environments, due to the formation of biofilm which is beneficial to maintaining water (Orvain et al., 2003). Moreover, the microbial community generally seemed to have the ability to adapt to, tolerate and recover quickly from desiccation and rewetting events (McKew et al., 2011). This hints the potential to create a relative stable micro-environment and improve the resilience of soils which could further support the plants and other benthos living there in coastal zones.

The barriers hindering a further development of biomorphodynamic, ecological and carbon frameworks mainly include a shortage of field data for model calibration and confirmation of simulation results (Arlinghaus et al., 2021). Existing modeling studies on large-scale morphological change induced by benthos are often only partly validated, *e.g.* by flume-scale experiments (Wood and Widdows, 2002; Van Prooijen and Winterwerp, 2010). Therefore, the data generated in this study enable further comparisons between model result and field measurement, which were usually limited to a few points in space and time in previous studies (Wood and Widdows, 2002; Lumborg et al., 2006).

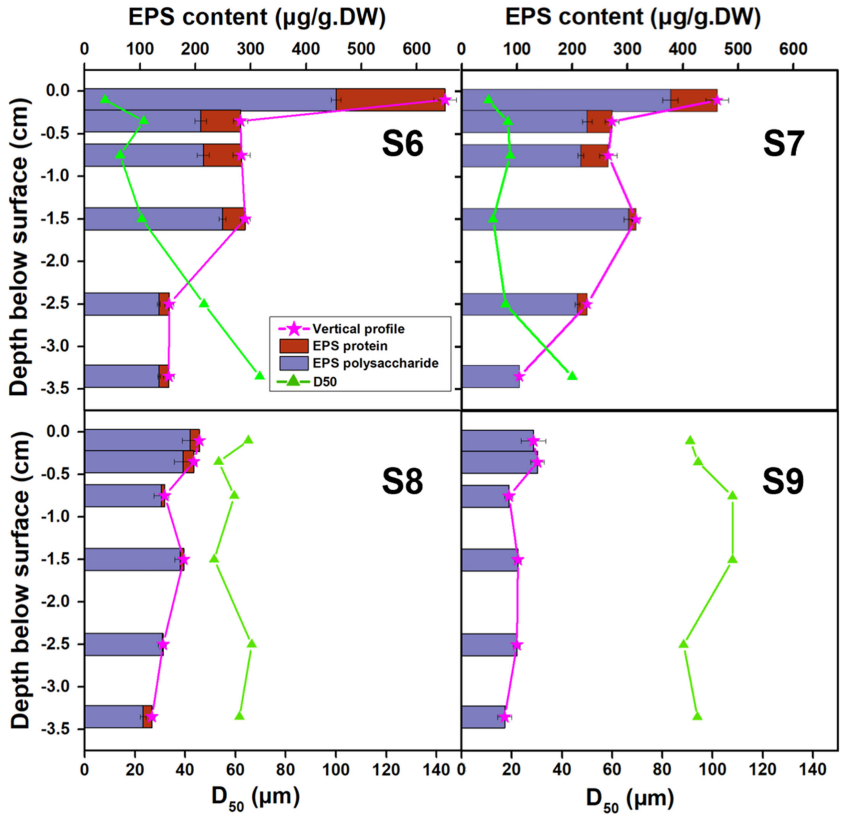

FIGURE 7
Comparison of vertical profiles of EPS content and grain size (D_{50}) for S6~S9 measured in June 2016.

Moreover, the variation of the microbial community across sites from land to sea and the variation with seasons both shows potential significance in predicting and coping with future environmental changings from the perspectives of preservation of gene pools. For instance, under the stress of sea level rise and global warming, the microbial community distribution (horizontal and vertical) in sediments may also reshape at the transition zone (quasi-abiotic-biotic); while the fate of the sediments and their associated microbial community is tightly related. High microbial diversity and rich gene pool are possibly conducive to the adaptive strategy of microbial community in changing environment, which awaits to be further explored. While this study could be the first step of the journey, further efforts on establishing the long-term database of the biological-physical contexture may be used as an early-predictor for the change of intertidal ecology under global changing and human activities. Collaborative work among hydraulic and sedimentation engineers as

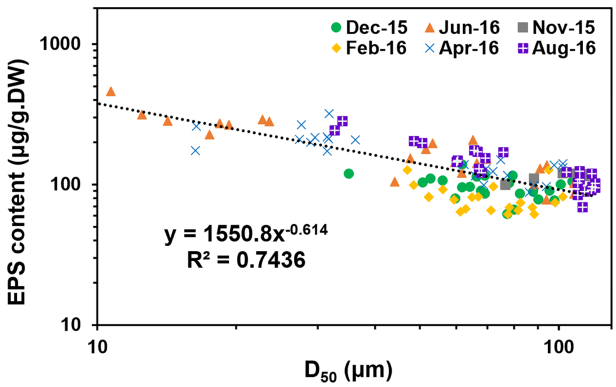

FIGURE 8
Correlation between the EPS content and grain size (D_{50}) based on the data collected at S6~S9 (6 layers stratified across 4 cm depth for each site) over 10 months (123 samples in total), R^2 =0.7436.

well as ecologists therefore awaits to be further established in this field where appropriate inter-disciplinary approaches are needed and mutual goals to be achieved (Gerbersdorf et al., 2020).

5 Conclusion

In this study, microbial activity was observed over a depth of 4 cm on Jiangsu tidal flats over 10 months. We demonstrated that the microbiological effects did not merely present on the surface, but greatly varied and stratified within the top 4 cm layer. This provided robust evidence for the co-existence of biofilms over intertidal system, and the penetration potential from the flat surface downwards inside the deeper bed. Detailed analysis further demonstrate that bacterial community structure showed a clear vertical variation with higher operational taxonomic unit (OTU) numbers at 1-2 cm depth than in the top 2 mm, probably because of the decreasing disturbance by hydrodynamic forces with sediment depth. However, the microbial production rates and metabolic activities, represented by extracellular polymeric substances (EPS) production, were always higher in the top layers. In addition, seasonal changes were strongly reflected in the vertical patterns of EPS but could not explain the variation across sites. The overall EPS secretion in spring and summer was generally at high level than that in autumn and winter, with the maximum value of 5~6 times higher. Nevertheless, the Scanning Electronic Images of the samples showed that even in winter, the micromorphology exhibited clearly formed biofilm-sedimentary matrix. Interestingly, the concentration of EPS was in good relationship to the grain size of their bound sediments (represented by the value of D_{50}), independent of temporal or spatial variation. With the decrease of the grain size, the EPS concentration increased exponentially. Despite the significant variation on microbial activity and sedimentary grain size individually, the basic relationship between EPS concentration and D_{50} however did not alter. Our results demonstrate that spatial scale (especially in depth) should be carefully considered when investigating ecological mechanisms that could be largely influenced by the sedimentary bio-physical contextures.

Data availability statement

The datasets presented in this study can be found in online repositories. The names of the repository/repositories and accession number(s) can be found below: Chen, Xindi (2023), "Biophysical contexture of coastal biofilm-sediments varies heterogeneously and seasonally at the centimeter scale across the bed-water interface", Mendeley Data, V1, doi: 10.17632/8mz8929fhn.1. Data and the results presented in this study can be obtained through Mendeley Data online (doi: 10.17632/8mz8929fhn.1).

Author contributions

Conceptualization: XC. Funding acquisition: YK, XC, QZ. Investigation: XC, CJ, KZ. Methodology: XC, QZ. Project Administration: YK. Resources: XC, YK. Writing – original draft: XC. All authors contributed to the article and approved the submitted version.

Funding

Funding for this project was provided by the National Key Research and Development Project, MOST, China (2022YFC3106204), the National Natural Science Foundation of China (52101318) and the Fundamental Research Funds for the Central Universities (B210202029).

Acknowledgments

Our thanks go to Jia Xu, Shibai Yu and all our group members for their assistance with the laboratory and field work.

Conflict of interest

The authors declare that the research was conducted in the absence of any commercial or financial relationships that could be construed as a potential conflict of interest.

Publisher's note

Supplementary material

The Supplementary Material for this article can be found online at: https://www.frontiersin.org/articles/10.3389/fmars.2023.1131543/full#supplementary-material

References

Amos, C. L., Droppo, I. G., Gomez, E. A., and Murphy, T. P. (2003). The stability of a remediated bed in hamilton harbour, lake ontario, canada. *Sedimentology* 50, 149–168. doi: 10.1046/j.1365-3091.2003.00542.x

Arlinghaus, P., Zhang, W., Wrede, A., Schrum, C., and Neumann, A. (2021). Impact of benthos on morphodynamics from a modeling perspective. *Earth Sci. Rev.* 221, 103803. doi: 10.1016/j.earscirev.2021.103803

Battin, T. J., Besemer, K., Bengtsson, M. M., Romani, A. M., and Packmann, A. I. (2016). The ecology and biogeochemistry of stream biofilms. *Nat. Rev. Microbiol.* 14, 251–263. doi: 10.1038/nrmicro.2016.15

Battin, T. J., Kaplan, L. A., Findlay, S., Hopkinson, C. S., Marti, E., Packman, A. I., et al. (2008). Biophysical controls on organic carbon fluxes in fluvial networks. *Nat. Geosci* 1, 95–100. doi: 10.1038/ngeo101

Battin, T. J., Kaplan, L. A., Newbold, J. D., and Hansen, C. M. E. (2003). Contributions of microbial biofilms to ecosystem processes in stream mesocosms. *Nature* 426, 439–442. doi: 10.1038/nature02152

Cai, Y., Liu, Z., Zhang, S., Liu, H., Nicol, G., and Chen, Z. (2022). Microbial community structure is stratified at the millimeter-scale across the soil–water interface. *ISME Commun.* 2, 53. doi: 10.1038/s43705-022-00138-z

Caporaso, J. G., Kuczynski, J., Stombaugh, J., Bittinger, K., Bushman, F. D., Costello, E. K., et al. (2010). Qiime allows analysis of high-throughput community sequencing data. *Nat. Methods* 7, 335–336. doi: 10.1038/nmeth.f.303

Chen, X., Zhang, C., Paterson, D., Thompson, C., Townend, I., Gong, Z., et al. (2017a). Hindered erosion: the biological mediation of noncohesive sediment behavior. *Water Resour Res.* 53, 4787–4801. doi: 10.1002/2016WR020105

Chen, X., Zhang, C., Paterson, D. M., Townend, I. H., Jin, C., Zhou, Z., et al. (2019). The effect of cyclic variation of shear stress on non-cohesive sediment stabilization by microbial biofilms: the role of 'biofilm precursors'. *Earth Surf Process Landf* 44, 1471–1481. doi: 10.1002/esp.4573

Chen, X., Zhang, C., Townend, I. H., Gong, Z., Feng, Q., and Yu, X. (2022). The resilience of biofilm-bound sandy systems to cyclic changes in shear stress. *Water Resour Res.* 58, e2021W–e31098W. doi: 10.1029/2021WR031098

Chen, X., Zhang, C., Townend, I., Paterson, D., Gong, Z., Jiang, Q., et al. (2021). Biological cohesion as the architect of bed movement under wave action. *Geophys Res. Lett.* 48, e2020G–e92137G. doi: 10.1029/2020GL092137

Chen, X., Zhang, C., Zhou, Z., Gong, Z., Zhou, J., Tao, J., et al. (2017b). Stabilizing effects of bacterial biofilms: eps penetration and redistribution of bed stability down the sediment profile. *J. Geophysical Research: Biogeosci.* 122, 3113–3125. doi: 10.1002/2017JG004050

de Brouwer, J. F. C., and Stal, L. J. (2001). Short-term dynamics in microphytobenthos distribution and associated extracellular carbohydrates in surface sediments of an intertidal mudflat. *Mar. Ecology-Progress Ser.* 218, 33–44. doi: 10.3354/meps218033

de Brouwer, J., Wolfstein, K., Ruddy, G. K., Jones, T., and Stal, L. J. (2005). Biogenic stabilization of intertidal sediments: the importance of extracellular polymeric substances produced by benthic diatoms. *Microb. Ecol.* 49, 501–512. doi: 10.1007/s00248-004-0020-z

Donlan, R. M., and Costerton, J. W. (2002). Biofilms: survival mechanisms of clinically relevant microorganisms. *Clin. Microbiol. Rev.* 15, 167. doi: 10.1128/CMR.15.2.167-193.2002

Douvere, F. (2021). Blue carbon can't wait. *Science* 373, 601. doi: 10.1126/science.abl7128

Edgar, R. C. (2010). Search and clustering orders of magnitude faster than blast. *Bioinformatics* 262460. doi: 10.1093/bioinformatics/btq461

Elbert, W., Weber, B., Burrows, S., Steinkamp, J., and Pöschl, U. (2012). Contribution of cryptogamic covers to the global cycles of carbon and nitrogen. *Nat. Geosci* 5, 459–462. doi: 10.1038/ngeo1486

Fagherazzi, S., FitzGerald, D., Fulweiler, R., Hughes, Z., Wiberg, P., and Shroder, J. F. (2013). *"Ecogeomorphology of tidal flats," in treatise on geomorphology* (San Diego: Academic Press), 201–220.

Fierer, N., and Jackson, R. B. (2006). The diversity and biogeography of soil bacterial communities. *Proc. Natl. Acad. Sci. U. S. A.* 103, 626–631.doi: 10.1073/pnas.0507535103

Gao, B., Zhu, X., Xu, C., Yue, Q., Li, W., and Wei, J. (2008). Influence of extracellular polymeric substances on microbial activity and cell hydrophobicity in biofilms. *J. Chem. Technol. Biotechnol.* 83, 227–232. doi: 10.1002/jctb.1792

Gerbersdorf, S. U., Koca, K., Debeer, D., Chennu, A., and Terheiden, K. (2020). Exploring flow-biofilm-sediment interactions: assessment of current status and future challenges. *Water Res.* 185, 116182. doi: 10.1016/j.watres.2020.116182

Gerbersdorf, S. U., and Wieprecht, S. (2015). Biostabilization of cohesive sediments: revisiting the role of abiotic conditions, physiology and diversity of microbes, polymeric secretion, and biofilm architecture. *Geobiology* 13, 68–97. doi: 10.1111/gbi.12115

Gobet, A., Boeer, S. I., Huse, S. M., van Beusekom, J. E. E., Quince, C., Sogin, M. L., et al. (2012). Diversity and dynamics of rare and of resident bacterial populations in coastal sands. *Isme J.* 6, 542–553. doi: 10.1038/ismej.2011.132

Hope, J. A., Malarkey, J., Baas, J. H., Peakall, J., Parsons, D. R., Manning, A. J., et al. (2020). Interactions between sediment microbial ecology and physical dynamics drive heterogeneity in contextually similar depositional systems. *Limnol Oceanogr* 65, 2403–2419. doi: 10.1002/lno.11461

Hunter, E. M., Mills, H. J., and Kostka, J. E. (2006). Microbial community diversity associated with carbon and nitrogen cycling in permeable shelf sediments. *Appl. Environ. Microbiol.* 72, 5689–5701. doi: 10.1128/AEM.03007-05

Jiao, N., Herndl, G. J., Hansell, D. A., Benner, R., Kattner, G., Wilhelm, S. W., et al. (2010). Microbial production of recalcitrant dissolved organic matter: long-term carbon storage in the global ocean. *Nat. Rev. Microbiol.* 8, 593. doi: 10.1038/nrmicro2386

Jin, C., Gong, Z., Shi, L., Zhao, K., Tinoco, R. O., San Juan, J. E., et al. (2022). Medium-term observations of salt marsh morphodynamics. *Front. Mar. Sci.* 9. doi: 10.3389/fmars.2022.988240

Li, T., Bai, R., and Liu, J. (2008). Distribution and composition of extracellular polymeric substances in membrane-aerated biofilm. *J. Biotechnol.* 135, 52–57. doi: 10.1016/j.jbiotec.2008.02.011

Li, J. S., Chen, X. D., Townend, I., Shi, B. W., Du, J. B., Gao, J. H., et al. (2021). A comparison study on the sediment flocculation process between a bare tidal flat and a clam aquaculture mudflat: the important role of sediment concentration and biological processes. *Mar. Geol* 434, 106443. doi: 10.1016/j.margeo.2021.106443

Liang, Z., Li, W., Yang, S., and Du, P. (2010). Extraction and structural characteristics of extracellular polymeric substances (eps), pellets in autotrophic nitrifying biofilm and activated sludge. *Chemosphere* 81, 626–632. doi: 10.1016/j.chemosphere.2010.03.043

Lowry, O. H., Rosebrough, N. J., Farr, A. L., and Randall, R. J. (1951). Protein measurement with the folin phenol reagent. *J. Biol. Chem.* 193, 265–275. doi: 10.1016/S0021-9258(19)52451-6

Lubarsky, H. V., Hubas, C., Chocholek, M., Larson, F., Manz, W., Paterson, D. M., et al. (2010). The stabilisation potential of individual and mixed assemblages of natural bacteria and microalgae. *PloS One* 5, e13794. doi: 10.1371/journal.pone.0013794

Lumborg, U., Andersen, T. J., and Pejrup, M. (2006). The effect of hydrobia ulvae and microphytobenthos on cohesive sediment dynamics on an intertidal mudflat described by means of numerical modelling. *Estuar. Coast. Shelf Sci.* 68, 208–220. doi: 10.1016/j.ecss.2005.11.039

Ma, T., Zhu, S., Wang, Z., Chen, D., Dai, G., Feng, B., et al. (2018). Divergent accumulation of microbial necromass and plant lignin components in grassland soils. *Nat. Commun.* 9, 3480. doi: 10.1038/s41467-018-05891-1

Mcclain, M. E., Boyer, E. W., Dent, C. L., Gergel, S. E., Grimm, N. B., Groffman, P. M., et al. (2003). Biogeochemical hot spots and hot moments at the interface of terrestrial and aquatic ecosystems. *Ecosystems* 6, 301–312. doi: 10.1007/s10021-003-0161-9

McKew, B. A., Taylor, J. D., McGenity, T. J., and Underwood, G. J. C. (2011). Resistance and resilience of benthic biofilm communities from a temperate saltmarsh to desiccation and rewetting. *ISME Joural* 5, 30–41. doi: 10.1038/ismej.2010.91

Murray, N. J., Phinn, S. R., DeWitt, M., Ferrari, R., Johnston, R., Lyons, M. B., et al. (2019). The global distribution and trajectory of tidal flats. *Nature* 565, 222. doi: 10.1038/s41586-018-0805-8

Oakes, J. M., Eyre, B. D., Middelburg, A., and Boschkerb, H. (2010). Composition, production, and loss of carbohydrates in subtropical shallow subtidal sandy sediments: rapid processing and long-term retention revealed by 13c-labeling. *Limnol. Oceanog.* 55, 39–40. doi: 10.4319/lo.2010.55.5.2126

Orvain, F., De Crignis, M., Guizien, K., Lefebvre, S., Mallet, C., Takahashi, E., et al. (2014). Tidal and seasonal effects on the short-term temporal patterns of bacteria, microphytobenthos and exopolymers in natural intertidal biofilms (brouage, france). *J. Sea Res.* 92, 6–18. doi: 10.1016/j.seares.2014.02.018

Orvain, F., Galois, R., Barnard, C., Sylvestre, A., Blanchard, G., and Sauriau, P. G. (2003). Carbohydrate production in relation to microphytobenthic biofilm development: an integrated approach in a tidal mesocosm. *Microb. Ecol.* 45, 237–251. doi: 10.1007/s00248-002-2027-7

Passarelli, C., Meziane, T., Thiney, N., Boeuf, D., Jesus, B., Ruivo, M., et al. (2015). Seasonal variations of the composition of microbial biofilms in sandy tidal flats: focus of fatty acids, pigments and exopolymers. *Estuar. Coast. Shelf Sci.* 153, 29–37. doi: 10.1016/j.ecss.2014.11.013

Paterson, D. M. (1989). Short-term changes in the erodibility of intertidal cohesive sediments related to the migratory behavior of epipelic diatoms. *Limnol Oceanogr* 34, 223–234. doi: 10.4319/lo.1989.34.1.0223

Paterson, D. M., and Daborn, G. R. (1991). *Sediment stabilisation by biological action: significance for coastal engineering* (Bristol, UK: University of Bristol Press).

Paterson, D. M., and Hope, J. A. (2021). "Diatom biofilms: ecosystem engineering and niche construction," in *Diatoms: Biology and applications*. Eds. S. Cohn, K. Manoylov and R. Gordon (USA: Scrivener Publishing), 135–158.

Perkins, R. G., Davidson, I. R., Paterson, D. M., Sun, H., Watson, J., and Player, M. A. (2006). Low-temperature sem imaging of polymer structure in engineered and natural sediments and the implications regarding stability. *Geoderma* 134, 48–55. doi: 10.1016/j.geoderma.2005.08.017

Perkins, R. G., Paterson, D. M., Sun, H., Watson, J., and Player, M. A. (2004). Extracellular polymeric substances: quantification and use in erosion experiments. *Cont Shelf Res.* 24, 1623–1635. doi: 10.1016/j.csr.2004.06.001

Raunkjaer, K., Hvitved-Jacobsen, T., and Nielsen, P. H. (1994). Measurement of pools of protein, carbohydrate and lipid in domestic wastewater. *Water Res.* 28, 251–262. doi: 10.1016/0043-1354(94)90261-5

Roche, K. R., Drummond, J. D., Boano, F., Packman, A. I., Battin, T. J., and Hunter, W. R. (2017). Benthic biofilm controls on fine particle dynamics in streams. *Water Resour. Res.* 53, 222–236. doi: 10.1002/2016WR019041

Rodriguez-Caballero, E., Belnap, J., Büdel, B., Crutzen, P. J., Andreae, M. O., Pöschl, U., et al. (2018). Dryland photoautotrophic soil surface communities endangered by global change. *Nat. Geosci* 11, 185–189. doi: 10.1038/s41561-018-0072-1

Rubol, S., Freixa, A., Carles-Brangari, A., Fernandez-Garcia, D., Romani, A. M., and Sanchez-Vila, X. (2014). Connecting bacterial colonization to physical and biochemical

changes in a sand box infiltration experiment. *J. Hydrol (Amst)* 517, 317–327. doi: 10.1016/j.jhydrol.2014.05.041

Schloss, P. D., Westcott, S. L., Ryabin, T., Hall, J. R., Hartmann, M., Hollister, E. B., et al. (2009). Introducing mothur: open-source, platform-independent, community-supported software for describing and comparing microbial communities. *Appl. Environ. Microbiol.* 75, 7537. doi: 10.1128/AEM.01541-09

Stone, M., Krishnappan, B. G., and Emelko, M. B. (2008). The effect of bed age and shear stress on the particle morphology of eroded cohesive river sediment in an annular flume. *Water Res.* 42, 4179–4187. doi: 10.1016/j.watres.2008.06.019

Sunil, S. A., and Lee, D. J. (2008). Extraction of extracellular polymeric substances from aerobic granule with compact interior structure. *J. Hazard. Mater* 154, 1120–1126. doi: 10.1016/j.jhazmat.2007.11.058

Thullner, M., and Baveye, P. (2010). Computational pore network modeling of the influence of biofilm permeability on bioclogging in porous media. *Biotechnol. Bioengineering* 99, 1337–1351. doi: 10.1002/bit.21708

Underwood, G. J. C., and Paterson, D. M. (1993). Seasonal changes in diatom biomass, sediment stability and biogenic stabilization in the severn estuary. *J. Mar. Biol. Assoc. U K* 73, 871–887. doi: 10.1017/S0025315400034780

Valentine, K., Hotard, A., Elsey-Quirk, T., and Mariotti, G. (2021). Benthic biofilm potential for organic carbon accumulation in salt marsh sediments. *Wetlands* 42 (1), 7. doi: 10.1007/s13157-021-01528-0

Van Prooijen, B. C., and Winterwerp, J. C. (2010). A stochastic formulation for erosion of cohesive sediments. *J. Geophys Res. Oceans* 115, C01005. doi: 10.1029/2008JC005189

Vert, M., Doi, Y., Hellwich, K. H., Hess, M., and Schué, F. (2012). Terminology for biorelated polymers and applications (iupac recommendations 2012). *Pure Appl. Chem.* 84. doi: 10.1351/PAC-REC-10-12-04

Vogt, M., Flemming, H. C., and Veeman, W. S. (2000). Diffusion in pseudomonas aeruginosa biofilms: a pulsed field gradient nmr study. *J. Biotechnol.* 77, 137–146. doi: 10.1016/S0168-1656(99)00213-8

Volk, E., Iden, S. C., Furman, A., Durner, W., and Rosenzweig, R. (2016). Biofilm effect on soil hydraulic properties: experimental investigation using soil-grown real biofilm. *Water Resour Res.* 52, 5813–5828. doi: 10.1002/2016WR018866

Waqas, A., Neumeier, U., and Rochon, A. (2020). Seasonal changes in sediment erodibility associated with biostabilization in a subarctic intertidal environment, st. Lawrence estuary, canada. *Estuar. Coast. Shelf Sci.* 245. doi: 10.1016/j.ecss.2020.106935

Wingender, J., Neu, T. R., and Flemming, H. C. (1999). *Microbial extracellular polymeric substances*: Springer Berlin Heidelberg. doi: 10.1007/978-3-642-60147-7

Wood, R., and Widdows, J. (2002). A model of sediment transport over an intertidal transect, comparing the influences of biological and physical factors. *Limnol Oceanogr* 47, 848–855. doi: 10.4319/lo.2002.47.3.0848

Wu, Z., Jiang, W., Zeng, L., and Fu, X. (2023). Theoretical analysis for bedload particle deposition and hop statistics. *J. Fluid Mech.* 954. doi: 10.1017/jfm.2022.959

Xu, F., Tao, J., Zhou, Z., Coco, G., and Zhang, C. (2016). Mechanisms underlying the regional morphological differences between the northern and southern radial sand ridges along the jiangsu coast, china. *Mar. Geol* 371, 1–17. doi: 10.1016/j.margeo.2015.10.019

Zhang, C. K., Zhang, D. S., Zhang, J. L., and Wang, Z. (1999). Tidal current-induced formation–storm-induced change–tidal current-induced recovery–interpretation of depositional dynamics of formation and evolution of radial sand ridges on the yellow sea seafloor. *Sci. China(Series D:Earth Sciences)* 42 (1) , 1–12. doi: 10.1007/BF02878492

Zhu, P., Chen, X., Zhang, Y., Zhang, Q., Wu, X., Zhao, H., et al. (2022). Porewater-derived blue carbon outwelling and greenhouse gas emissions in a subtropical multi-species saltmarsh. *Front. Mar. Sci.* 9. doi: 10.3389/fmars.2022.884951